Growing Robotic Endoscope for early Breast Cancer Detection: Robot Motion Control

Carmen Larrea[1], Pierre Berthet-Rayne[2], S.M.Hadi Sadati[2], Daniel Richard Leff[3], Christos Bergeles[2], and Ioannis Georgilas[1]

[1] Department of Mechanical Engineering, University of Bath, Bath, UK,
[2] Robotics and Vision in Medicine Lab, School of Biomedical Engineering & Imaging Sciences, King's College London, UK.
[3] Hamlyn Centre for Robotic Surgery and Imperial College Healthcare NHS Trust, UK.
i.georgilas@bath.ac.uk

Abstract. The direct relationship between early-stage breast cancer detection and survival rates has created the need for a simple, fast and cheap method to detect breast cancer at its earliest stages. Endoscopic evaluation of the mammary ducts known as ductoscopy has great potential to detect early breast cancers. Unfortunately, there are technical limitations, most notably lack of steerability and high tissue damage, limiting its practicality. A promising alternative to rigid endoscopy tools is the use of soft robots.

This paper presents the computational multidomain model for the MAMMOBOT soft growing prototype. The prototype is using pressurised saline solution to achieve elongation in the breast's ductal tree, a tendon driven catheter for steering, and an active channel for soft material storage. The derivation of the model is based on plant cell expansion, and physical modelling of the actuation and hydraulic systems.

The model is validated in 1D using experimental data from the MAMMOBOT prototype. All unknown model variables were identified during a parameter investigation using Latin Hypercube Sampling. The developed hydraulic model predicted the measured elongation with a 1.7mm RMSE error, 3.5% of the total robot length, while the combined actuation and hydraulic models predicted the elongation with 2.5mm RMSE, 5% of total length.

The results presented here is the first attempt to implement the growing robot concepts in small scales and demonstrate their accuracy. The developed model will be used to improve the closed loop control of the growing robot, improving steerability and positional accuracy, enhancing the cancer detection process.

Keywords: Soft Robotics, Hydraulic actuation, Robot Control.

1 Introduction

Breast cancer is the most common type of cancer in the UK with more than 55 thousand cases diagnosed every year[1] and with a 5-year mortality rate of 15%. For years, doctors and investigators have searched for ways of decreasing mortality through early detection. When diagnosed in its early stages 98% of people will survive breast cancer for 5 years or more against a 26% survival rate with a late-stage diagnosis [1].

These statistics highlight the importance of a procedure that will diagnose breast cancer in its earliest stages.

In its earliest form (stage 0) cancer is known as Ductal Carcinoma in Situ (DCIS). The detection of DCIS could increase the chances of survival of the patient and could even avoid the need for chemotherapy or surgical intervention. Current methods have numerous limitations such as being expensive, time-consuming or have reduced sensitivity and specificity[2]. For example, mammography screening is relatively inefficient in detecting DCIS as it only detects those tumours associated with calcifications which are less than 50% of all DCIS cases[3]. Considering 80-90% of breast cancers start developing as DCIS, a high number of cases go undetected or present as invasive cancers downstream.

Ductoscopy facilitates early diagnosis through the use of an endoscope which accesses the mammary ducts via the nipple in order to have a visual of the tumour[4]. Rigid endoscopes, however, are difficult to manipulate and cause significant strain on the surrounding tissue. This inflexibility means that the ductoscopy procedure is not yet widely used. Most MI tools currently have steerable tips but their length stops them from achieving optimal dexterity and stability when they reach the surgical site[5]. A good solution to overcome these challenges is the use of soft robotics as endoscopic tools since they can exploit their high flexibility to reach the target[6].

Robotic surgery has been a reality in the medical field for some time, but it is only relatively recently that soft robots have been adopted for use in surgical procedures. In 1997 Frazer [7] patented a worm-like robot to be used as a colonoscopy tool. Since then, many doctors and surgeons have realised the advantages that come with the use of a precise, manoeuvrable, and flexible tool in MI procedures. A technique that has shown great potential for catheter use is that of concentric tube robots[8]. This technology overcomes the difficulty in steering by the use of concentric pre-curved super elastic tubes which can form complex 3D shapes.

Another promising soft robotic technology that has shown potential is that of growing robots [9]. Their use has been investigated in many applications such as search and rescue, exploration of coral reefs [10] or archaeological sites [11], as well as medical procedures[12]. These robots are inspired by plant growth and elongate through eversion using air pressure inside a thin membrane. The MAMMOBOT project [13] explores using a growing robot as a ductoscopy tool, with the key novelty being the significant reduction of size allowing it to flexibly navigate the mammary duct system.

One of the common complexities for this class of robots is the modelling description of their behaviour to ensure safe and reliable control. The preferred methods of modelling come from nature given the similarities between robots and plants. One proposed approach is to use plant growth-inspired models for motion generation[14] while another is to draw inspiration from biological models of apical extension and mechanical models of compliant Bowden cable actuation[15].

The work presented here is building on existing apical models, extending them to match the structure and characteristics of the MAMMOBOT robot. The proposed model incorporates the unique features of the robot and offers modelling of the actuation system and the impact on robot growth and control. The final result is a step towards accurate operation of miniature growing robots.

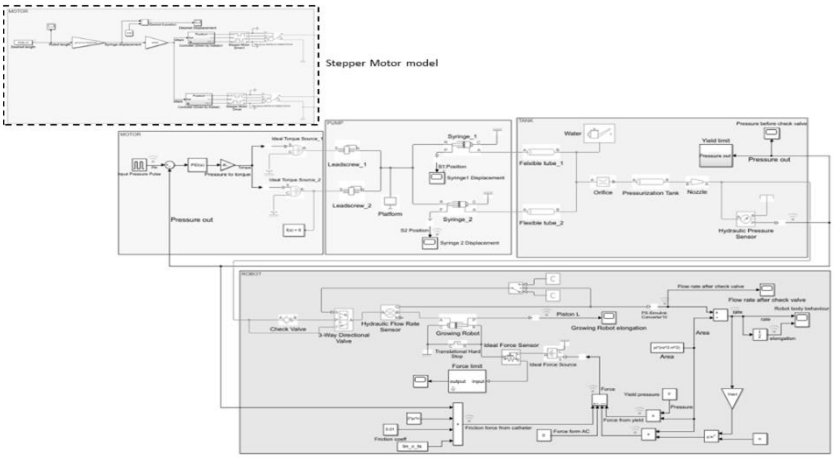

Fig. 1. Simulink multidomain model of MAMMOBOT. Green is the (generic) torque source model (dashed insert: stepper motor), yellow is the mechanical model of the syringe pump, blue is the hydraulic elements of the pressure tank, and purple is the growing element model.

2 Methods

There are three key methodical aspects in this study, firstly the development of the proposed model consisting of the actuation system, the hydraulic system and the growing robot element. Secondly, the data analysis metric for comparison of experimental and compuational results, and thirdly the parameter investigation for the unknown model parameters.

2.1 Actuation & Hydraulics Model

The actuation and hydraulics model is following the physical MAMMOBOT prototype developed by Berthet-Rayne et al. [13] and presented in green, yellow and blue in **Fig. 1**. It consists of a syringe pump (mechanical domain model) powered by a motor (electrical domain model) and a custom pressurized tank (hydraulic domain model) that supplies pressure to the growing robot. To simplify the actuation model the physical implementation of the catheter and the active channel were not included in this work.

Motor Model. Two different models for the motor were created to allow investigation of different model aspects. In the first instance the motor is modelled as an ideal torque source ensuring a direct control of the applied pressure. This model allows for the evaluation of different motors and relies on pressure sensing. This model is presented with green in **Fig. 1** and is connected to the rest of the model. The demanded pressure (P_d) is provided as an input and the equivalent torque is calculated by the characteristics of the pressure source, the syringe in this case:

$$T_d = \frac{P_d \times l_{lead} \times A_{syringe}}{2\pi} \tag{1}$$

where l_{lead} is the lead of the syringe pump lead screw, T_d the torque, and $A_{syringe}$ the cross-sectional area of the syringe plunger.

This model is a forward dynamic model and is used with experimental pressure measurements for model validation. To maintain the desired pressure, a closed loop PID controller is implemented and the feedback loop from the tank pressure can be seen in **Fig. 1**. The PID controller is tuned manually as (K_P=80, K_I =25 and K_D=0.5).

The second version of the motor model was based on the stepper motor used in the MAMMOBOT prototype. In this case the existing Simscape stepper motor model and driver was used[16]. This is an inverse kinematic model with which the desired growing robot length is an input and the motor achieves the desired pressure required to obtain that length. This is done in two steps, from the desired length of the robot to syringe displacement and then to stepper motor steps. The conversion from the length of the robot to syringe displacement assumes there are no fluid losses and the fluid is incompressible thus the relationship between syringe and robot pressures and volumes:

$$\frac{L_{syringe}}{L_{robot}} = \frac{A_{syringe}}{A_{robot}} \tag{2}$$

where, $L_{syringe}$ is the displacement of the syringe pump plunger, L_{robot} is the desired length of the robot and A_{robot} is the cross-section area. For the conversion from the length to the steps for the motor the dimensions of the lead screw for the plunger are used.

Syringe Pump Model. The pump subsystem is formed by available Simscape elements that can be seen in yellow in **Fig. 1**. The motors are driving lead screws which are coupled via a carrier platform with the syringe plungers The syringes were modelled using single acting cylinder blocks as they have the same functions and underlying equations. The function of this subsystem is to generate fluidic pressure which will be transmitted to the pressurized tank.

Pressurized Tank Model. The pressurization tank used in the MAMMOBOT prototype is custom made and an approximation has to be made as seen with blue in **Fig. 1** . A hydraulic pipeline with a non-circular cross-section was used. The tank has two top nozzles, one for pressure sensing and another for hydraulic pressurisation connected to the syringe pump. Hydraulic pressure is applied from the syringes to the tank through flexible hydraulic pipelines and an orifice. The flexible hydraulic pipelines in the model represent the silicone tubes that connect the syringe and the tank. The flexible property will cause some pressure absorption. The tank ends in a nozzle to which one end of the growing robot membrane is attached; this was modelled through the use of a gradual area change block. The nozzle outputs fluid into the growing robot with a pressure sensor measuring at this point.

The hydraulic fluid used in the MAMMOBOT robot is 0.9%NaCl saline water, which is the most common solution in medical applications. The differences in the mechanical properties of saline solution and water are negligible and therefore the system was modelled using pure water.

The detailed Simscape model and image of the experimental setup can be found at Robot model github page.

2.2 Growing robot Model

The growing robot modelling is based on the apical model described by Blumenschein et al. [15] and gives the pressure force (PA) of the robot as:

$$PA = \left[YA + \left(\frac{1}{\phi}v\right)^{\frac{1}{n}}A\right] + \left[\mu_s \omega L + C_e^{\frac{\mu_c L_i}{R_i}}\right] \tag{3}$$

where, Y is the yield pressure below which no growth happens, $\left(\frac{1}{\phi}v\right)^{\frac{1}{n}}A$ is a velocity term due to the material's resistance to elongation, $\mu_s \omega L$ is a friction term from outside contacts of the robot and $C_e^{\frac{\mu_c L_i}{R_i}}$ is a term due to the curvature of the robot. The first two terms are path independent and the latter two are path dependent and relate to the environment.

Equation 3 must be adapted for the MAMMOBOT robot. The introduction of a catheter tool through the centre of the growing robot will cause a friction force. The friction term in (3) can be substituted by the friction between the catheter and the growing robot. Assuming that the catheter moves forward relative to the growing robot this will result in a forward friction force (F_{fr}) in the growing robot which will accelerate its growth:

$$F_{fr} = PA \times 2\pi \times r_i \times L_c \times \mu_{rc} \tag{4}$$

where r_i is the radius of the catheter, L_c is the length of the catheter in contact with the robot and μ_{rc} is the coefficient of friction between the catheter and the robot. The dependence on length makes the force a path-dependent term.

The MAMMOBOT design introduces the use of an active channel that has the ability to exert a force (F_{AC}) on the growing robot in order to better control the elongation behaviour and is thus path-independent. As a result of this and (4), (3) becomes:

$$PA = \left[YA + \left(\frac{1}{\phi}v\right)^{\frac{1}{n}}A + F_{AC}\right] + \left[-F_{fr} + C_e^{\frac{\mu_c L_i}{R_i}}\right] \tag{5}$$

It must be noted that no friction term has been added for the interaction of the growing robot with the walls of the ducts (lumen). As explained above, one of the main advantages of the growing robot technique is its ability to elongate without relative movement between the body and its environment. The friction between the growing robot and the lumen can therefore be neglected.

Since (5) is written in terms of forces it was concluded that an ideal single-acting cylinder could be used to model the robot in the Simulink environment. The underlying equations which govern the single-acting cylinder are:

$$F_{cyl} = A_{pis}P_{in} \quad \text{and} \quad q = A_{pis}v \tag{6}$$

where F_{cyl} is the force developed by the cylinder, A_{pis} is the piston area and P_{in} is the pressure at the cylinder inlet. The term q represents flow rate and v represents velocity.

The forces from (5) can be substituted into (6) to calculate the force into the single-acting cylinder. In this study, the growing robot is analysed in straight paths only, while the velocity can be substituted from (6). The resulting force equation is:

$$F_{cyl} = \left[YA + \left(\frac{q}{\phi A}\right)^{\frac{1}{n}} A + F_{AC} \right] + \left[-F_{fr} \right] \tag{7}$$

This force is modelled in Simulink as an ideal force source to the single-acting cylinder, acting against elongation as it is a resistive force. The length data for the friction force from (4) is obtained from experimental catheter displacement data as the model created has not simulated catheter behaviour. The force from the active channel will remain zero for this work as it was not used to apply force during the experiment.

In order to ensure safety a pressure limit is introduced to prevent yield failure of the growing robot membrane. To make a stress analysis of the robot, the growing robot element is considered as a thin pressure vessel. Due to the low ratio of thickness to radius, an approximation can be made to assume that the membrane experiences negligible radial stress when pressurized and only experience longitudinal(σ_L) and circumferential (σ_θ) stress will be considered. Failure due to yielding in the robot membrane will be caused when the circumferential stress reaches the yield stress (σ_y)[17]. The maximum permitted pressure is therefore described by:

$$P_{max} = \frac{2t\sigma_y}{r_o} \tag{8}$$

The membrane material in this case is LDPE with a yield stress value of 40MPa. The growing element has a thickness (t) of 35μm with an outer radius (r_o) of 1.5mm and an inner radius of (r_i) of 0.45mm. With a safety factor of 5 the maximum pressure was calculated to be 373.3kPa. This limit was added as a simulation stop limit in the model.

The initial resistance of the growing robot to elongation due to the Yield Pressure was modelled hydraulicly as a check valve after the pressure tank and before the growing element. This approach is useful for setting a pressure limit below which no flow occurs and acts as a static pressure resistance. Because this approach will prevent unidirectional flow, a three-way directional valve is used to override the check valve when the flow changes direction. The valve is controlled based on the flow direction as detected through the use of a flow rate sensor. After the initial pressure is overcome the Yield Pressure term is added via the single-acting cylinder and (7).

2.3 Data analysis

The evaluation of the model was performed by comparing model predicted results for robot elongation, flow and pressure with experimental observations as collected via the work by Berthet-Rayne et al. [13]. The comparison was performed using the Root Mean Square Error (RMSE).

2.4 Parameter Investigation

Equation 7 has three main unknown parameters that have to be found empirically: yield pressure, extensibility and n term. The values were found using the computational model and the experimental data available, through a parameter investigation. This was

done by determining the set of values that will give a model response most closely approximates the experimental data. Through the use of Latin Hypercube Sampling (LHS) a distribution of 500 parameter sets were obtained. The different combinations of values are then inputted into the system and the RMSE value is calculated to identify which parameter combination gives a result that simulates the behaviour of the experimental data most closely. The ideal torque source version of the model was used to perform this analysis.

3 Results & Discussion

The model developed above was validated with the single run data from the work by Berthet-Rayne et al. [13] to evaluate accuracy but more repeats are needed for evaluating repeatability. Both versions of the motor model were tested, i.e. the model using the ideal torque source to drive the leadscrew and the model using the stepper motor. Prior to validation tests the parameter investigation was done to identify the unknown parameters of the system and based on those validate the models.

3.1 Parameter Investigation

Figure 2 presents the results from the parameter investigation for the three parameters identified in (7). The 3D graph shows all 500 points generated using LHS. The ranges for the random generation were selected following an initial manual sampling investigation of the wider parameter space. The effect of each parameter on the outcome was analysed in order to obtain the range that would most affect RMSE. Parameter *n* is a scaling power term close to unity and therefore a range of 0.9 to 1.1 was selected. A Yield Pressure, i.e. before growth can commence, range of 5kPa-15kPa was selected while an extensibility, i.e. the ability of the robot to extent, range of 4000-10000$Pa^{-n}m/s$ was selected. The table in **Fig. 2** gives the values achieving the minimum RMSE which will be used for the validation tests.

The parameter with the most significant effect on RMSE is yield pressure since the RMSE value greatly changes along that axis. It can be observed that the optimal yield pressure value is around 8kPa. This is expected as a change in the resistive force acting against elongation would affect the rate of growth of the robot. On the other hand, for extensibility and *n term* it can be observed that there is no clear correlation between either of them and the RMSE value. Considering that extensibility and *n term* are part of the velocity term in (7), a high value in the extensibility term will greatly reduce the effect of this force on the growing robot which will also mean that the *n term* effect will be reduced as well.

3.2 Model Validation

For the validation two assumptions are made, first, the model takes into account the movement of the robot in 1D only i.e., extension, ignoring curvature. Therefore, only experimental data of extension are being used. The second assumption has to do with the application of the pressure experimentally. As explained in [13], no pressure control was performed but a “duty cycle controller” was used of no pressure-pressure.

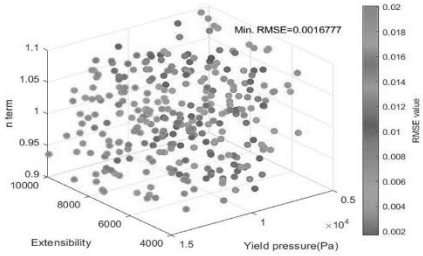

Identified Terms
Yield Pressure (Y)
7.9kPa
Extensibility
$7.6x10^3$ $Pa^{-n}m/s$
n
1.07

Fig. 2. Parameter Investigation Results. The 500 points generated with the LHS are presented, with the color scale being the RMSE value. On the right the identified values are given.

Growing robot validation. In the validation of the growing robot model with the ideal torque model, the duty cycle pressure demand for the *Growing Cycle*, thus a pulse pressure signal of 0 to 150kPa, is the demand to the model and the elongation of the robot was observed and compared to the experimental results as shown **Fig 3**. The pressure was controlled via the closed-loop PID controller.

In this experiment it can be observed that the robot length is shown to follow the same behaviour as the experimental length data, **Fig. 3**. The overall rate of growth for both is similar, reaching a length of 50mm in 10 seconds. An RMSE value of 1.7mm corresponds to a total error of 3.4% of the final length of the growing robot. This is a promising result, for surgical robotic applications aim for a 1-2mm accuracy [18]. Analysing both elongation signals, it can be observed that the experimental data has bigger peaks than the model data. The biggest variation occurs in the positive gradient of the peak sections, the experimental data has a higher rate of growth. Contrastingly the retracting section of the peak is larger and less steep than in the model. The lower negative gradient could be attributed to a pulling force from the active channel that is not included in the model currently. It must also be noted that there is no experimental pressure data available to confirm the actual pressure applied to the robot. This uncertainty surrounding the experimental pressure could mean the input pressure was representative, causing the differences in gradients. The catheter movement (not modelled) could also have had an unexpected effect on the growing robot behaviour causing some material to fold or buckle.

Actuation system validation. The validation of the actuation system was done by using as stepper motor demand the desired growing robot length using equation (2) and the length-to-stepper motor steps conversion. The pressure generated was recorded as well as the model predicted vs the desired growing robot length, **Fig. 4.**

The actuation system model is overall less accurate. However, the length response can still be seen to follow a similar pattern to the experimental observations. The pressure response to the length inputs has a faster triangular frequency which can be attributed to the stepper motor as it actuates the syringe pump. Nonetheless, the predicted robot length produced from this pressure is smoother than the observed length and the error is still low, and the overall rate of growth is similar reaching a length of 50mm in 10 seconds.

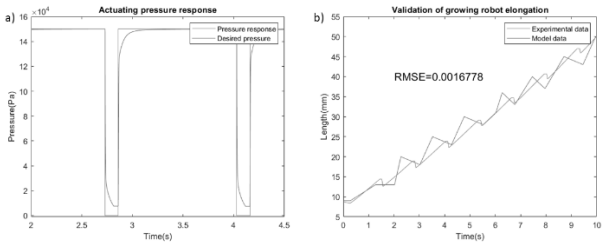

Fig. 3. Growing Robot Model Validation. a) Demand and response of the actuating pressure b) Growing robot length data model predicted and experimental.

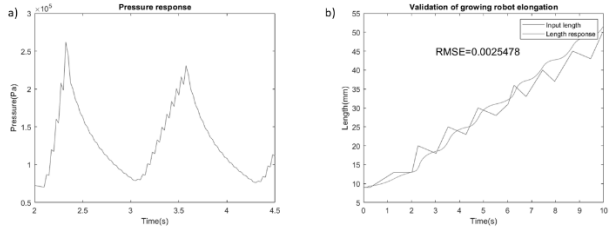

Fig. 4. Actuation Model Validation a) Pressure response to the demanded length. b) Growing robot length response compared to the desired length.

An RMSE of 2.5mm means that there is a 5% error compared to the final length of the robot. It must be noted that there is no pressure feedback loop to correct for losses and variations caused by the system. It can still be observed that there are advancements and retraction by the robot at approximately the same rate as the observed behaviour. There is a time lag in between demand and response which can be associated with viscous frictional losses across the actuation system.

4 Conclusion

This work introduces a computational model for the MAMMOBOT robot, a novel growing robot for early breast cancer detection which aims to serve as an endoscopy tool entering the ductal network via the nipple. The multidomain model was created and validated using experimental observations and the results showed that the prediction of growth behaviour was accurate for both an ideal torque actuator and the stepper motor used in the experiments. The former resulted in an RMSE error of 1.7mm while the latter of 2.5mm, at 3.5% and 5% of the total length of the robot.

In this work the basis for an accurate analytical model to describe the behaviour of the MAMMOBOT device was created, however, more repeatability assessment of the result is needed. More investigation is needed on the effect of curvature in the robot when expanding the model from 1D to 2D and 3D. Moreover, in its current form the model ignores the active channel and the guiding catheter but from initial observations a detailed analysis of their impact needs to be conducted. Finally, investigations should also look into how the addition of sensing instrumentation such as multiple pressure and flow sensors will complement the model for control.

The successful development of the MAMMOBOT device could be incredibly valuable in the field of breast cancer diagnosis. The successful computational model of the first prototype which was presented in this paper will aid in achieving a precise motion and control of the robot increasing detection accuracy.

Acknowledgments

This work is being supported by Cancer Research UK (CRUK) via the MAMMOBOT– A flexible robot for early breast cancer diagnosis grant.

References

1. Cancer Research UK. Breast cancer statistics.
2. Mokbel, K. & Cutuli, B. Heterogeneity of ductal carcinoma in situ and its effects on management. *Lancet Oncology* vol. 7 756–765 (2006).
3. Breast cancer in women - Diagnosis - NHS.
4. Mokbel, K., Escobar, P. F. & Matsunaga, T. Mammary ductoscopy: current status and future prospects. doi:10.1016/j.ejso.2004.10.004.
5. Polygerinos, P. *et al.* Soft Robotics: Review of Fluid-Driven Intrinsically Soft Devices; Manufacturing, Sensing, Control, and Applications in Human-Robot Interaction. *Adv. Eng. Mater.* **19**, (2017).
6. Cianchetti, M. & Menciassi, A. Soft robots in surgery. *Biosyst. Biorobotics* **17**, 75–85 (2017).
7. Frazer, R. E. Apparatus for Endoscopic Examination United States Patent, Patent Number: 4,176,662. (1979).
8. Bergeles, C. *et al.* Concentric tube robot design and optimization based on task and anatomical constraints. *IEEE Trans. Robot.* **31**, 67–84 (2015).
9. Hawkes, E. W., *et al.* A soft robot that navigates its environment through growth. *Sci. Robot.* **2**, 1–8 (2017).
10. Luong, J. *et al.* Eversion and retraction of a soft robot towards the exploration of coral reefs. in *2nd IEEE Inter. Conf. on Soft Robotics* (RobSoft), 801–807 (2019).
11. Coad, M. M. *et al.* Vine Robots: Design, Teleoperation, and Deployment for Navigation and Exploration. *IEEE Robot. Autom. Mag.* **27**, 120–132 (2020).
12. Slade, P. *et al.* Design of a soft catheter for low-force and constrained surgery. *IEEE Int. Conf. Intell. Robot. Syst.* **2017-Septe**, 174–180 (2017).
13. Berthet-Rayne, P. *et al.* MAMMOBOT: A miniature steerable soft growing robot for early breast cancer detection. *IEEE Robot. Autom. Lett.* 1–8 (2021).
14. Wooten, M., *et al.* Exploration and inspection with vine-inspired continuum robots. in *Proceedings - IEEE Inter. Conf. on Rob. and Autom. (ICRA)* 5526–5533 (2018).
15. Blumenschein, L. H., Okamura, A. M. & Hawkes, E. W. Modeling of Bioinspired Apical Extension in a Soft Robot. in *Conf. on Biom. and Bioh. Sys.* 522–531 (2017).
16. Lyshevski, S. E. *Electromechanical systems, electric machines, and applied mechatronics*. (CRC Press, 2018).
17. Godaba, H., *et al.* Payload capabilities and operational limits of eversion robots. in *Lecture Notes in Computer Science (*vol. 11650 LNAI 383–394 (Springer Verlag, 2019).
18. Haidegger, T. *et al.* Spatial accuracy of surgical robots. in *Proceedings - 2009 5th International Symposium on Applied Computational Intelligence and Informatics, SACI 2009* 133–138 (2009).